4728 *Macromolecules* **2009**, *42*, 4728–4738
DOI: 10.1021/ma9006544

Macromolecules
ARTICLE

Mechanical Properties and Elastic Behavior of Syndiotactic Propene−Butene Copolymers

Claudio De Rosa,* Finizia Auriemma, Marco Corradi, Ludovica Caliano, Odda Ruiz de Ballesteros, and Rocco Di Girolamo

Dipartimento di Chimica "Paolo Corradini", Università di Napoli "Federico II", Complesso Monte S.Angelo, Via Cintia, 80126 Napoli, Italy

Received October 25, 2008; Revised Manuscript Received May 9, 2009

ABSTRACT: The mechanical properties of syndiotactic propylene−butene copolymers (sPPBu), prepared with a metallocene catalyst, have been studied in the whole range of comonomer composition. Melt-crystallized unoriented films and oriented fibers of sPPBu copolymers show good elastic properties even though the samples present non-negligible level of crystallinity at any comonomer composition. These materials behave as thermoplastic elastomers with remarkable rigidity and mechanical strength that can be tuned by changing the comonomer composition. In samples with low butene concentration the elastic properties are associated with the reversible transformation between the trans-planar form III of syndiotactic polypropylene, obtained by stretching, and the helical form II, formed by releasing the tension. The occurrence of reversible phase transitions assists the elasticity of these materials through a non-negligible free energy contribution that is added to the conventional entropic contribution.

Introduction

One of the most successful achievements of metallocene catalytic systems for polymerization of olefins is the possibility of promoting the copolymerization of 1-alkenes, with production of materials with unprecedented chain microstructures and unexpected physical and mechanical properties. For instance, novel elastomeric materials based on stereoblock polypropylene,[1] poorly isotactic polypropylene[2] and propylene−ethylene copolymers,[3] block copolymers formed by crystallizable isotactic or syndiotactic polypropylene blocks and amorphous ethylene−propylene copolymers block,[4] multiblock ethylene−octene copolymers,[5] syndiotactic polypropylene,[6] and syndiotactic copolymers of propylene with other olefins[7−14] have recently been obtained with different classes of metallocene catalysts. In the case of syndiotactic polypropylene (sPP)[6] and syndiotactic copolymers of propene with other olefins,[7−14] a wealth of new elastomeric materials that present high molecular mass and properties ranging from those of nearly amorphous weak rubbers to those of stiff elastomers, with a high degree of crystallinity and high melting temperature, may be obtained.[6,13] In particular, it has been shown that elasticity and high crystallinity may become compatible in the same material if crystals play an active role in the elastic recovery and do not merely act as physical cross-links of the amorphous network.[6,13] When crystals actively participate to the elastic mechanism, elasticity can develop in spite of high stiffness and high crystallinity.[6,13]

The archetypal example of this category of "crystalline elastomers" is sPP.[6] The active role of crystals in the elasticity of highly stereoregular sPP samples is due to the occurrence of a reversible polymorphic transition of the metastable form III with chains in trans-planar conformation,[6,15] obtained by stretching into the more stable form II with chains in helical conformation,[6,16] which develops when the tensile stress is released.[6] Elasticity in highly stereoregular sPP is not merely entropic as in conventional elastomers but also partially due to an enthalpic contribution provided by the reversible martensitic-like crystal−crystal phase transition between form III and form II.[6] Because of the high level of crystallinity, the values of the Young modulus in sPP are quite high, typical of crystalline thermoplastic materials rather than those of elastomers.[6] Weaker elastomers may be obtained by decreasing the degree of crystallinity, which, in turn, may be achieved by decreasing the degree of stereoregularity of sPP, through the use of different catalytic systems in the polymerization process. Because of the low crystallinity, the enthalpic contribution plays a progressively less important role in the elasticity of low stereoregular sPP, and elasticity in these weak elastomers becomes merely entropic. The fine-tuning of the stiffness of elastomeric materials by tuning the crystallinity has also been demonstrated for syndiotactic propylene−ethylene copolymers, through the control of ethylene concentration.[13] These studies have introduced the concept of "enthalpic elasticity",[6] which is exhibited by elastomeric materials that experience both plastic and elastic responses and is due to reversible polymorphic transformations occurring during plastic deformation. The "enthalpic elasticity" is different from the "entropic elasticity" of conventional elastomers, which is due to the transformations between extended and random coil conformations of chains in the amorphous state, and from the Hookean elasticity, exhibited by any solid material in the range of linear elastic deformation (before the yield point).

The crystallization behavior of syndiotactic copolymers of propylene with butene (sPPBu) has recently been studied.[14] These copolymers crystallize in the whole range of composition in disordered modifications[14] intermediate between the *B*-centered form I of sPP[17,18] and the *C*-centered form I of syndiotactic poly(1-butene) (sPB)[19] (or the *C*-centered form II of sPP),[1,16] which are characterized by similar modes of packing of 2/1 helical chains. In this paper the mechanical properties of sPPBu copolymers are studied in detail and are correlated with the polymorphic transformations occurring during stretching and relaxation. The "enthalpic" and "entropic" elasticity exhibited by these materials during plastic deformation are discussed as a function of the copolymer composition.

*To whom correspondence should be addressed: Tel +39 081 674346; Fax +39 081 674090; e-mail claudio.derosa@unina.it.

 Published on Web 06/05/2009

Table 1. Composition, Intrinsic Viscosity ([η]), Average Molecular Mass (M_v), Melting Temperature of As-Prepared and Aged Samples (T_m), and Glass transition Temperature (T_g) of sPPBu Copolymers[a]

samples	gas composition (mol % of 1-butene)	copolymer composition (mol % of 1-butene)[b]	[η] (dL/g)[c]	M_v[d]	T_m (°C)[e]	T_g (°C)[f]
sPPBu1	1.1	3.2	2.6	349 000	138	0
sPPBu2	2.6	6.1	2.0	266 000	126	−0.8
sPPBu3	4.8	6.7	2.5	335 000	123	−0.1
sPPBu4	6.6	11.2	2.3	307 500	110	−4.1
sPPBu5	7.6	13.6	3.0	405 500	108	−2.9
sPPBu6	11.0	18.2	2.1	279 600	100	−4.9
sPPBu7	16.5	31.5	2.0	266 000	85	−7.1
sPPBu8	22.6	37.9	1.50	197 000	71	−8.0
sPPBu9	34.6	51.7	1.46	191 500	70	−10.3
sPPBu10	45.2	52.1	1.35	176 500	64	−10.7
sPPBu11	65.1	69.9	1.10	142 600	57	−13.5
sPPBu12	84.7	89.0	1.65	217 500	54	−16.9

[a] Polymerization temperature = 10 °C; pressure = 1 atm; solvent = toluene (100 mL); molar ratio Al/Zr = 1000; catalyst amount = 2−3 mg; reactor volume = 250 mL; polymerization time = 2 h; flow rate = 0.3 L/min; yield = 2−5 g. [b] Determined from ^{13}C NMR spectra. [c] Measured in 1,2,3, 4-tetrahydronaphthalene solutions at 135 °C. [d] Molecular masses evaluated from values of intrinsic viscosity. [e] Determined from DSC curves of as-prepared and aged samples recorded at heating rate 10 °C/min. [f] Determined from the DSC heating curves at 10 °C/min of samples crystallized from the melt by cooling at 10 °C/min.

Experimental Section

Samples of sPPBu copolymers with a content of 1-butene in the range 0−100 mol % were synthesized with a single center syndiospecific catalyst composed of (phenyl)$_2$methylen(cyclopentadienyl)(9-fluorenyl)zirconium dichloride and methylaluminoxane (MAO) with the method described in ref 14.

All copolymerizations were run at 10 °C in a 250 mL Pyrex reactor, agitated with magnetic stirrer, containing toluene (100 mL) and MAO. Gas mixtures of 1-butene and propene at the appropriate composition, prepared with vacuum line techniques and standardized by gas chromatography, were bubbled through the liquid phase at atmospheric pressure and a flow rate of 0.3 L/min. The polymerization was started by syringing in a toluene solution of the catalyst (2−3 mg), and the Al/Zr molar ratio was adjusted to 1000. Under such conditions, total monomer conversions were lower than 15%, this ensuring a nearly constant feeding ratio. The copolymers were coagulated with excess methanol acidified with enough HCl (aqueous, concentrated) to prevent the precipitation of alumina from MAO hydrolysis, filtered, washed with further methanol, and vacuum-dried. Typical yields were 2−5 g with a 120 min reaction time. The conditions of polymerization and the composition of all sPPBu samples are reported in Table 1.

The used catalyst is highly syndiospecific and regioselective (the amount of regioirregularities due to 2,1 insertions of propylene units being less than 0.1%).[6] Furthermore, the presence in the catalyst of the Ph_2C bridge, instead of the Me_2C bridge of the classic Ewen−Razavi C_s-symmetric catalyst (isopropylildene)(cyclopentadienyl)(9-fluorenyl)zirconium dichloride,[20] allows achieving higher molecular weights when used in the same polymerization conditions.[21]

The composition of the copolymers was determined by analysis of the ^{13}C NMR spectra, according to the method suggested in ref 22. NMR spectra were recorded with a Varian XL-200 spectrometer operating at 50.3 MHz, of 10% w/v polymer solutions in deuterated tetrachloroethane (also used as internal standard) at 120 °C. The copolymers, according to this analysis, are random and homogeneous in the composition. The melting temperatures were obtained with a differential scanning calorimeter Perkin-Elmer DSC-7 performing scans in a N_2 atmosphere at heating rate of 10 °C/min. The intrinsic viscosities were measured in 1,2,3, 4-tetrahydronaphthalene solutions at 135 °C, using a standard Ubbelohde viscosimeter. The viscosity-average molecular masses of sPPBu samples were obtained from values of intrinsic viscosity using the parameters of the Mark−Houwink equation reported for atactic polypropylene, $\alpha = 0.96$ and $k = 1.24\ 10^{-5}$ dL/g.[23]

Unoriented films used for structural and mechanical analysis have been obtained by compression-molding of as-polymerized samples. Powders of sPPBu samples have been heated at temperatures 20−30 °C higher than the melting temperature of the as-prepared samples under a press at very low pressure, kept at this temperature for 10 min, and slowly cooled to room temperature.

X-ray powder diffraction profiles have been obtained with an automatic Philips diffractometer using a Ni-filtered Cu Kα radiation. The crystallinity has been evaluated from the X-ray powder diffraction profiles by the ratio of the crystalline diffraction area and the total area of the diffraction profile. The crystalline contribution has been obtained by subtracting the X-ray diffraction profile of the amorphous phase from the whole diffraction profile. For samples with butene concentration lower than 30 mol % that crystallize by cooling the melt to room temperature, the amorphous halo has been obtained from the X-ray diffraction profile of atactic polypropylene after suitable scaling. For samples with butene concentration higher than 30 mol % that are amorphous soon after cooling the melt to room temperature, the amorphous haloes of each samples have been obtained from the X-ray diffraction profiles of the compression-molded amorphous samples soon after the cooling from the melt.

Mechanical tests have been performed at room temperature on compression-molded films and stress-relaxed oriented films of the samples sPPBu with a miniature mechanical tester apparatus (Minimat, by Rheometrics Scientific), following the standard test method for tensile properties of thin plastic sheeting ASTM D882-83. Rectangular specimens 10 mm long, 5 mm wide, and 0.3 mm thick of the compression-molded films have been stretched up to the break or up to a given strain $\varepsilon = 100(L_f - L_0)/L_0$, with L_0 and L_f the initial and final lengths, respectively.

Two benchmarks have been placed on the test specimens and used to measure elongation. The values of the tension set and elastic recovery have been measured on compression-molded films after a given strain ε or after breaking according to the standard test method ASTM D412-87. For breaking experiments, specimens of initial length L_0 have been stretched up to the break. Ten minutes after breaking the two pieces of the sample have been fit carefully together so that they are in contact over the full area of the break, and the final total length L_r of the specimen has been obtained by measuring the distance between the two benchmarks. The tension set at break has been calculated as $t_b = 100(L_r - L_0)/L_0$.

Stress-relaxed oriented fibers have been prepared by stretching at room temperature specimens of compression-molded films of initial length L_0 up to final lengths L_f equal to 3.5−5.5 times the initial length L_0, that is, up to a maximum deformation ε_{max} of 250−450% ($\varepsilon_{max} = 100(L_f - L_0)/L_0$), keeping the film under tension for 10 min and then removing the tension allowing the

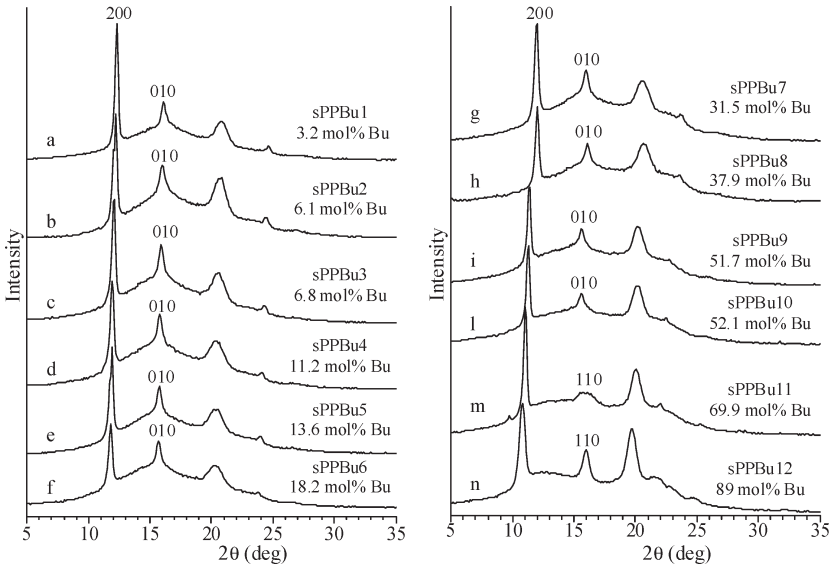

Figure 1. X-ray diffraction profiles of compression-molded films slowly crystallized from the melt of sPPBu samples of the indicated butene (Bu) concentration. The 200 and 010 reflections of the disordered *B*-centered form I of sPP and the 110 reflection of the *C*-centered form II of sPP of sPB are indicated. For samples sPPBu7−sPPBu12 with butene contents higher than 30 mol %, the diffraction profiles of the compression-molded samples crystallized by aging at room temperature for long time are reported.

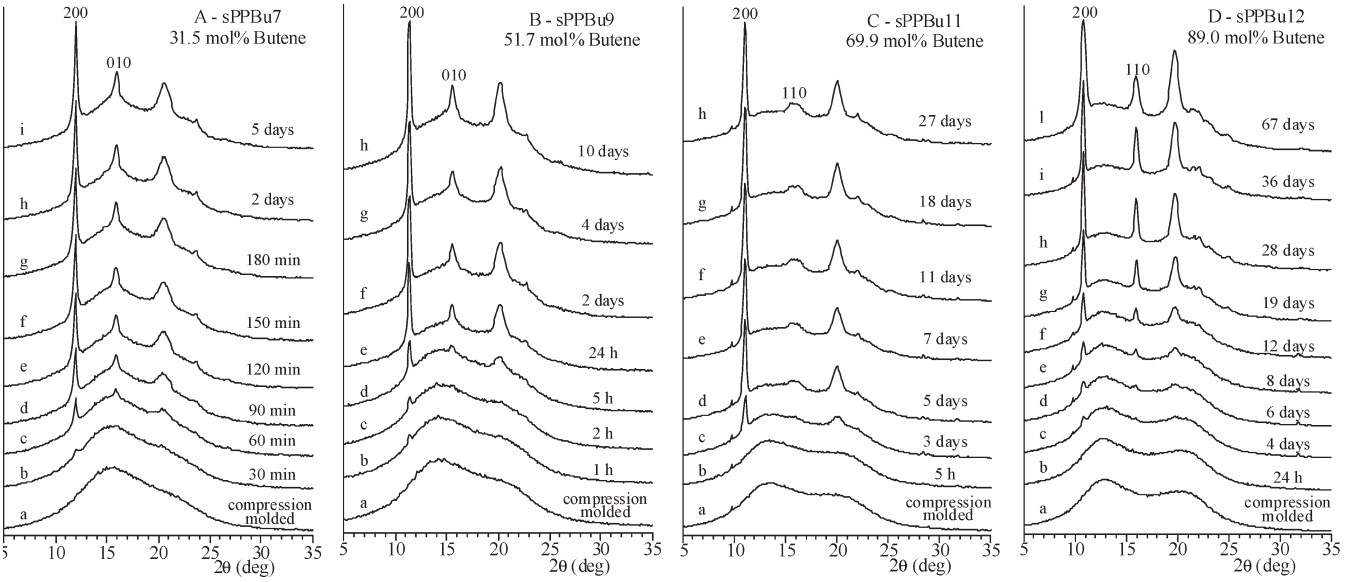

Figure 2. X-ray powder diffraction profiles of compression-molded samples of sPPBu copolymers with butene concentration higher than 30 mol % slowly cooled from the melt to room temperature and aged at room temperature for the indicated aging time.

relaxation of the sample up to the length L_r. The final length of the relaxed specimens L_r is measured after 10 min. For each sample the relaxed length L_r is generally lower than the length L_f achieved during the stretching but higher than the initial length L_0 because the elastic recovery of the unoriented films after removing the tension is not complete. The tension set and elastic recovery are calculated as $t_s(\varepsilon) = 100(L_r - L_0)/L_0$ and $r(\varepsilon) = 100(L_f - L_r)/L_r$, respectively, whereas the percentage of the total strain that is recovered after releasing the tension $(L_f - L_0)$ is obtained as $R = 100(L_f - L_r)/(L_f - L_0) = 100(\varepsilon - t_s(\varepsilon))/\varepsilon$. Oriented fibers of samples sPPBuN stress-relaxed from ε_{max} = 250, 300, 400, or 450% deformations are identified as samples sPPBu-N-ε_{max}. Mechanical cycles of stretching and relaxation have been performed at room temperature on these stress-relaxed films, and the corresponding hystereses have been recorded. In these cycles the stress-relaxed fibers having the new initial length L_r have been stretched up to the final lengths $L_f = 3.5L_0$, $4L_0$, $5L_0$, or $5.5L_0$ (that is, up to the maximum length achieved during the stretching of the starting unoriented films), so that the deformation achieved during the cycles is $\varepsilon = 100(L_f - L_r)/L_r$ and is lower than ε_{max} (being in the range 40−100%). This precaution was taken in order to avoid further irreversible plastic deformations during the stretching steps. After each cycle, the values of the tension set have been measured. The final length of the relaxed specimens L_r' has been measured 10 min after the end of the relaxation step, and the tension set has been calculated as $t_s(\varepsilon) = 100(L_r' - L_r)/L_r$.

Results and Discussion

Crystallization Behavior. The X-ray powder diffraction profiles of compression-molded samples of sPPBu copolymers cooled from the melt and aged at room temperature for several days are shown in Figure 1. These copolymers are crystalline in the whole range of comonomer composition

due to the complete cocrystallization of butene and propylene in the crystalline lattices of sPP and sPB.[14] Samples with butene content higher than 30 mol % are amorphous just after cooling the melt (profiles a of Figure 2) but crystallize by aging at room temperature for several days (Figure 2). The crystallinity of these samples are reported in Figure 3 as a function of the aging time. It is apparent that the crystallization rate decreases with increasing butene content.

The values of melting temperatures of as-prepared and compression-molded samples, the glass transition temperature, and the crystallinity achieved for all samples after crystallization at room temperature are reported in Figure 4 as a function of butene concentration. The melting temperature regularly decrease with increasing butene content from the value of 155 °C of sPP[6] to that of nearly 50 °C of sPB.[19] The crystallinity of compression-molded samples is lower than that of the as-prepared samples aged at room temperature for several months. This indicates that, even for the samples with low butene concentration that crystallize from the melt, only a partial crystallization occurs by cooling the melt to room temperature, and the long time aging at room temperature produces further crystallization. For compression-molded samples that have been used for the analysis of the mechanical properties, only a small and smooth decrease of the crystallinity is observed with increasing butene concentrations up to a large minimum value of nearly 25−30% in the range of butene concentration of 40−60 mol %, and then a slight increases is observed for further increase of butene content (Figure 4B).

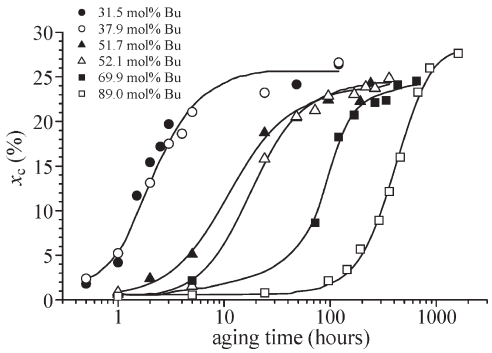

Figure 3. Degree of crystallinity of compression-molded samples of sPPBu copolymers with butene concentration higher than 30 mol % slowly cooled from the melt to room temperature and aged at room temperature as a function of the aging time.

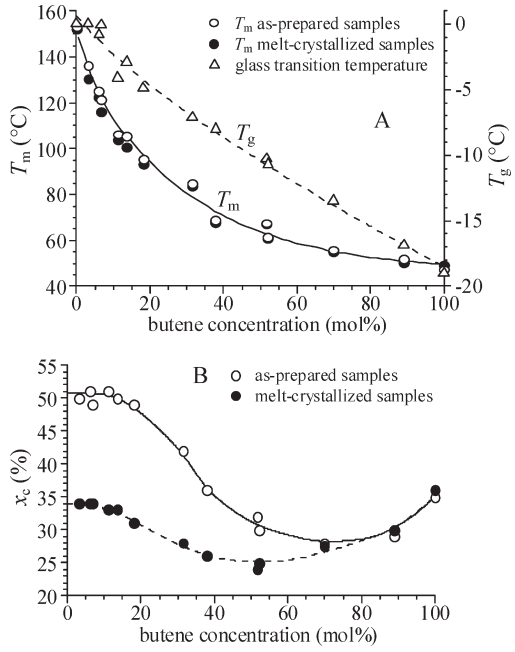

Figure 4. Melting temperature (○,●), glass transition temperature (△) (A), and degree of crystallinity (○,●) (B) of as-prepared (○) and melt-crystallized compression-molded (●) samples of sPPBu copolymers as a function of butene concentration. The values of the glass transition temperatures have been determined from the DSC heating curves at 10 °C/min of samples crystallized from the melt by cooling at 10 °C/min. The melting temperatures and the degrees of crystallinty of samples of sPP and sPB homopolymers are taken from the literature.[6,]

The data of Figures 1−4 indicate that samples of sPPBu copolymers crystallize from the melt or from the amorphous phase (Figure 2) in disordered modifications intermediate between the *B*-centered form I of sPP (Figure 5A)[17,18] and the *C*-centered form I of sPB (Figure 5B).[19] In fact, the diffraction peak in the range of $2\theta = 15°-16°$ is interpreted as a 010 reflection, typical of the *B*-centered mode of packing of Figure 5A, in the diffraction profiles a-l of Figure 1 of the samples sPPBu1−sPPBu10 or as a 110 reflection, typical of the *C*-centered mode of packing of form I of sPB of Figure 5B or form II of sPP,[16] in the diffraction profiles *m*, *n* of Figure 1 of the samples sPPBu11−sPPBu12. Therefore, samples with butene contents lower than nearly 70 mol % crystallize in disordered modifications close to the form I of sPP (Figure 5A), whereas samples with higher butene content crystallize in disordered modifications close to the form I of sPB (Figure 5B).[14]

The exact values of the Bragg angles of the 200 reflection in the range of $2\theta = 10.5°-12.2°$ and of the 010 or 110 reflection at $2\theta = 15°-16°$ depend on the butene concentration. The values of the *a* and *b* axes of the orthorhombic unit cells increase with increasing butene content from the values typical of form I of sPP (Figure 5A)[17] to those of form I of sPB (Figure 5B) (Table 2 of ref 14). This indicates that both comonomeric units are included in the unit cells of the two homopolymers.

In all sPPBu samples, a large amount of structural disorder is present in the crystals. The absence of any diffraction peak at $2\theta = 18°-19°$ in the X-ray powder diffraction profiles of Figure 1, corresponding to the 211 reflection of the limit ordered form I of sPP (space group *Ibca*),[17] also indicates the presence of disorder in the positioning of

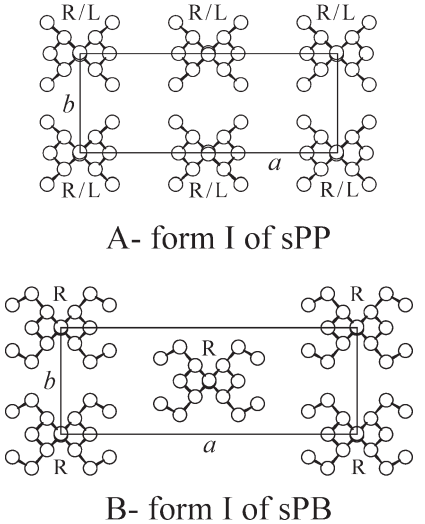

Figure 5. Limit disordered models of packing of form I of sPP (A, space group *Bmcm*) and limit ordered model of form I of sPB (B, space group $C222_1$) (R = right-handed, L = left-handed).

right- and left-handed helical chains in each site of the lattice of sPP (as in the disordered model of Figure 5A).[24]

Mechanical Properties. The stress−strain curves of compression-molded films of the sPPBu samples after being achieved the maximum crystallinity by aging at room temperature for long time (Figure 1) are reported in Figure 6 in comparison with the curve of a highly stereoregular sample of sPP homopolymer prepared with the same catalyst.[6] The most important mechanical parameters evaluated from the stress−strain tests are reported in Table 2 and in Figure 7 as a function of butene concentration.

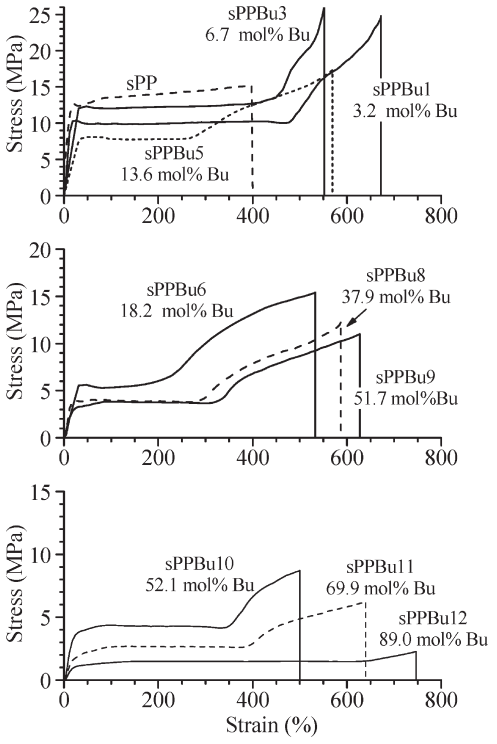

Figure 6. Stress−strain curves of compression-molded films of sPPBu copolymer samples of the indicated concentration of butene (Bu) comonomeric units.

All sPPBu samples do not deform homogeneously, and generally, necking is observed. They can be easily stretched up to values of deformation of 500−700%. The values of stress at any strain gradually decrease with increasing butene content, reflecting a gradual increase of flexibility and decrease of resistance to the plastic deformation going from sPP to sPB. Furthermore, all sPPBu samples experience strain hardening at high deformations, starting from values of strain of 200−300%. As recently shown in our previous paper,[25] at these deformations the crystals of all samples have already achieved a high degree of orientation with chain axes parallel to the stretching direction. This produces a remarkable increase of the mechanical strength at higher deformations (Figure 6).

The Young's modulus, the stress at yield, and the stress at break decrease with increasing butene content (Figure 7A,B) according to the smooth decrease of crystallinity (Figure 4B). The values of strain at yield are nearly constant (≈34%) for all butene concentrations, whereas the strain at break slightly increases with increasing butene content (Figure 7C). These data indicate that sPPBu samples become less rigid and more easily deformable with increasing butene content. The uniform decrease of the mechanical strength and the smooth increase of the compliance with increasing butene concentration reflect the easy inclusion of comonomeric units (propene and butene) in the crystals of the two homopolymers (sPB and sPP).[14] This produces an almost uniform distribution of the comonomeric units in the amorphous and crystalline regions of sPPBu copolymers, resulting in a gradual change of the mechanical properties.

The ductility of sPPBu copolymers is, however, much lower than that of analogous syndiotactic propene−ethylene copolymers (sPPEt).[13] We recall, indeed, that in the case of sPPEt samples even a small content of ethylene units induces a dramatic increase of ductility,[13] with values of deformation at break higher than 2000% and much higher than those generally observed for sPP homopolymer samples prepared with the same catalyst and showing similar stereoregularity and crystallinity.[13] It has been shown that ethylene units are partially included in the crystals of sPP and induce conformational kink-band disorder with formation of highly defective crystals of the helical form II of sPP. Therefore, the

Table 2. Young Modulus (E), Strain (ε_y) and Stress at Yield (σ_y), Strain (ε_b) and Stress at Break (σ_b), Tension Set at Break (t_b), Percentage of the Strain That Is Recovered after Breaking (R_b), and Degree of Crystallinity of Compression-Molded Films of sPPBu Copolymer Samples Compared with the Values of sPP and sPB Homopolymers

samples	1-butene content (mol %)	E (MPa)	ε_y (%)	σ_y (MPa)	ε_b (%)	σ_b (MPa)	t_b (%)	R_b (%)	x_c (%)[a]
sPP	0	256 ± 20	22 ± 2	13 ± 2	400 ± 20	15 ± 1	300 ± 10	25	40
sPPBu1	3.2	89 ± 13	18.1 ± 0.2	10.3 ± 0.9	672 ± 46	25 ± 3	290 ± 12	57	34
sPPBu2	6.1	78 ± 5	33 ± 1	12 ± 1	597 ± 90	25 ± 1	239 ± 36	60	34
sPPBu3	6.7	70 ± 6	31 ± 2	12 ± 2	552 ± 48	26 ± 4	150 ± 27	73	34
sPPBu4	11.2	54 ± 7	30.7 ± 0.2	6.8 ± 0.2	480 ± 13	15 ± 1	119 ± 34	75	33
sPPBu5	13.6	43 ± 6	32 ± 2	8 ± 1	570 ± 44	17 ± 4	151 ± 27	74	33
sPPBu6	18.2	41 ± 6	31.3 ± 0.4	5 ± 1	533 ± 70	15 ± 2	148 ± 14	72	31
sPPBu7	31.5	24 ± 2	22 ± 2	3.0 ± 0.8	592 ± 31	15 ± 1	144 ± 18	75	0
sPPBu7	31.5	25 ± 4	34 ± 2	5.8 ± 0.3	459 ± 49	10.9 ± 0.9	138 ± 25	70	28
sPPBu8	37.9	15 ± 4	24 ± 2	2.4 ± 0.5	698 ± 96	13 ± 2	142 ± 9	80	0
sPPBu8	37.9	19 ± 3	29 ± 2	3.9 ± 0.3	586 ± 62	12 ± 3	135 ± 13	77	26
sPPBu9	51.7	4 ± 1	26 ± 3	1.1 ± 0.3	663 ± 79	10.0 ± 0.8	167 ± 7	75	0
sPPBu9	51.7	11 ± 2	32 ± 4	3.2 ± 0.2	627 ± 28	11.0 ± 0.5	152 ± 8	76	24
sPPBu10	52.1	0.6 ± 0.1	72 ± 4	0.5 ± 0.1	878 ± 38	8.9 ± 0.9	333 ± 38	62	0
sPPBu10	52.1	12 ± 2	33 ± 2	3.8 ± 0.4	500 ± 30	8.7 ± 0.4	140 ± 13	72	25
sPPBu11	69.9	0.19 ± 0.02	98 ± 5	0.26 ± 0.04	1065 ± 45	3.8 ± 0.5	397 ± 34	63	0
sPPBu11	69.9	3.3 ± 0.3	34 ± 4	2.5 ± 0.2	644 ± 56	6.2 ± 0.4	150 ± 12	77	28
sPPBu12	89.0	> 0.1	99 ± 5	0.28 ± 0.02	1151 ± 151	0.6 ± 0.2	449 ± 59	61	0
sPPBu12	89.0	1.2 ± 0.1	37 ± 2	1.4 ± 0.3	747 ± 24	2.3 ± 0.1	148 ± 29	80	30
sPB	100	1.3 ± 0.3	44 ± 3	1.1 ± 0.2	730 ± 75	3.0 ± 0.9	14 ± 9	98	36

[a] For samples with butene concentrations higher than 30 mol % the mechanical parameters of amorphous samples (x_c = 0), evaluated from the stress−strain curves of compression-molded films recorded before the crystallization at room temperature, are also reported.

much higher ductility of sPPEt copolymers, compared to that of sPPBu copolymers, is related to the higher intrinsic flexibility of the sPPEt copolymer chains, which contain portions in the trans-planar conformation,[13] and the presence of more defective crystals.[13]

The values of tension set at break t_b of sPPBu copolymers are much lower than the values of deformation at break (Figure 7D and Table 2), and for all samples the percentage of the strain that is recovered after breaking is $R_b = 70-80\%$ (Table 2 and Figure 7E), much higher than that observed for the highly stereoregular sPP homopolymer sample (25%). This indicates that all sPPBu copolymer samples show remarkable elastic recovery after breaking. The tension set and the percentage of the recovered strain have also been evaluated for samples stretched up to a maximum deformation ε_{max} and then relaxed by removing the tension (Figure 7E). It is apparent that the percentage of strain that is recovered by releasing the tension from ε_{max} is very similar for all samples and tends to increase with increasing the maximum deformation achieved by stretching, indicating

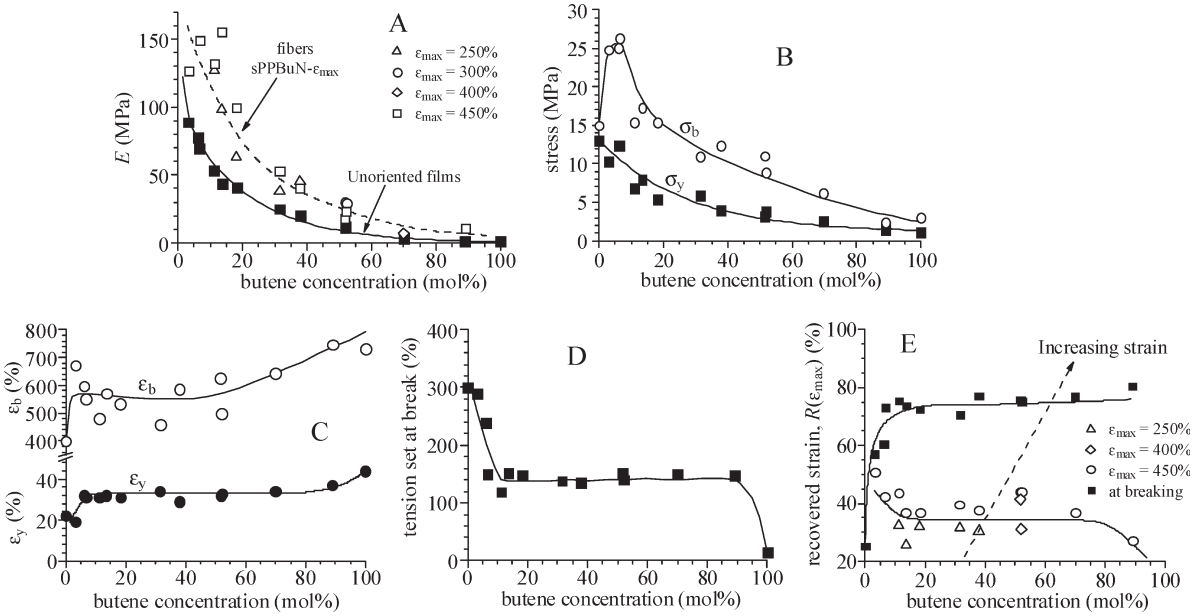

Figure 7. Values of Young's modulus (A), stress at yield (σ_y) and at break (σ_b) (B), strain at yield (ε_y) and at break (ε_y) (C), tension set at break (t_b) (D) and percentage of strain recovered $R(\varepsilon_{max})$ after stretching up to the break or to a maximum value of strain ε_{max} and then relaxed by removing the tension (E) of compression-molded films of sPPBu samples as a function of butene content. In (A) the values of Young's modulus of stress-relaxed fibers of sPPBu samples obtained by stretching compression-molded films up to a maximum value of strain ε_{max} and then removing the tension, after having experienced at least three consecutive hysteresis cycles (Figure 9) are also reported.

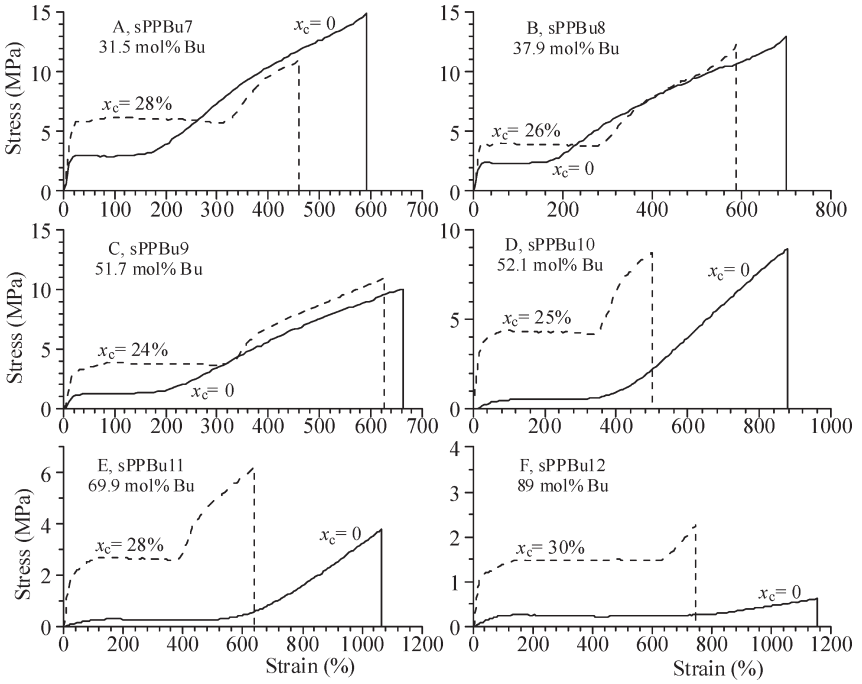

Figure 8. Stress–strain curves of compression-molded amorphous films of sPPBu copolymer samples of butene (Bu) concentration in the range 31–89 mol %, before the crystallization at room temperature (continuous lines) and after the complete crystallization by aging at room temperature (dashed lines). The values of crystallinity x_c are indicated.

that the elastic recovery is more important than the irreversible plastic deformation. These data demonstrate that in all sPPBu samples a given deformation is mostly recovered after removing the tension. Samples with butene content lower than 4 mol % present high melting temperatures (≈130 °C, Figure 4A) and behave as stiff thermoplastic elastomers like high stereoregular sPP,[6] even though the stress−strain curves present the typical shape of thermoplastic materials with well-defined yielding (Figure 6A) rather than that of elastomers.

sPPBu samples with butene content higher than 70 mol % present low melting temperatures (≈60 °C, Figure 4A) and behave as soft elastomers with still a good level of crystallinity (Figure 4B). Copolymer samples with butene content comprised in the range 4−70 mol % have intermediate values of melting temperatures (Figure 4A) and show mechanical properties gradually changing from that of rigid elastomers to that of soft elastomers, while maintaining a non-negligible level of crystallinity.

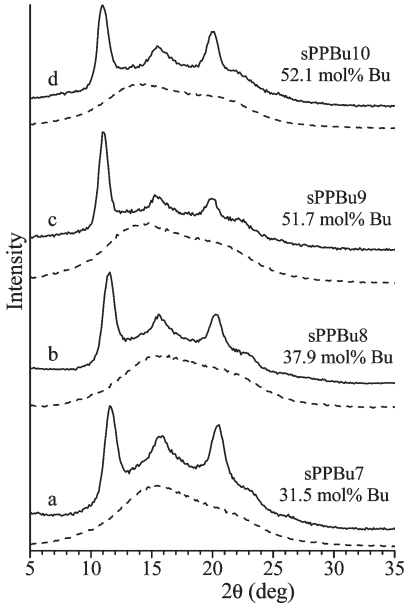

Figure 9. X-ray powder diffraction profiles of compression-molded amorphous films of samples sPPBu7−sPPBu10 before the stress−strain experiments of Figure 8 (dashed lines) and after the stretching up to the breaking in the tests of Figure 8 (continuous lines). In order to guarantee a random orientation of crystals in the stretched samples, the diffraction profiles of the stretched samples have been collected after having cut the films in small pieces immediately after breaking.

As shown in Figure 2, samples of sPPBu copolymers with butene concentration higher than 30 mol % are amorphous soon after the compression molding and cooling to room temperature and slowly crystallize by aging at room temperature for several days. The stress−strain curves of amorphous compression-molded specimens of some samples of copolymers sPPBu7−sPPBu12 before the crystallization at room temperature (samples of curves a of Figure 2) are reported in Figure 8 and compared with the stress−strain curves of the same samples after the complete crystallization at room temperature (data of Figure 6). The values of the mechanical properties for the amorphous samples are compared in Table 2 with those of the crystalline samples. It is apparent that the amorphous samples show values of Young's modulus, stress at yielding, and stress at low values of strain lower than those in the stress−strain curves of the same samples after the crystallization. The values of stress at breaking, instead, are nearly the same for the amorphous and the completely crystallized samples, in the case of sPPBu samples with lower butene content (in the range 31−60 mol %, samples sPPBu7−sPPBu10) (Figure 8A−D), whereas they increase with increasing crystallinity for the samples sPPBu11 and sPPBu12 with higher butene concentration (Figure 8E,F). Moreover, the values of the percentage of the strain recovered after breaking are in the range 75−80% for the samples sPPBu7−sPPBu9 and decrease slightly to nearly 60% for the samples sPPBu10−sPPBu12 (Table 2). These data indicate that even the amorphous samples show remarkable elastic properties.

In summary, amorphous samples present behavior of elastomeric materials with low modulus and low values of stress at low deformations and remarkable strain hardening at higher values of deformation, up to achieve values of stress at breaking similar to those of the crystalline materials. This increase of stress at high deformation is probably related to the crystallization during stretching, so that the stress−strain curves of amorphous samples become similar to those of the crystalline samples at high deformations.

It should be noticed that the amorphous samples of copolymers sPPBu7−sPPBu9 show evident yield point and

Table 3. Values of Tension Set ($t_s(\varepsilon_{max})$) and Elastic Recovery ($r(\varepsilon_{max})$) of Unoriented Compression-Molded Films of sPPBu Samples Stretched up to Deformations ε_{max} and Then Relaxed by Removing the Tension (So That Stress-Relaxed Oriented Fibers sPPBuN-ε_{max} Are Prepared) and Values of the Tension Set (t_s) and Percentage of Dissipated Energy (E_{dissip}) Measured after the First Hysteresis Cycle of the Type of Figure 10

sample	butene (mol %)	ε_{max} (%)	$t_s(\varepsilon_{max})$ (%)	$r(\varepsilon_{max})$ (%)	$t_s^{I\ cycle}$ (%)[a]	$E_{dissip}^{I\ cycle}$ (%)	$E_{dissip}^{II-III\ cycles}$ (%)
sPPBu1	3.2	450	223 ± 3	67 ± 3	10 ± 1	38 ± 2	28 ± 2
sPPBu3	6.7	450	260 ± 9	53 ± 4	12 ± 2	45 ± 3	27 ± 3
sPPBu4	11.2	250	169 ± 21	30 ± 10	1.7 ± 0.6	34 ± 5	27.1 ± 4
sPPBu4	11.2	450	255 ± 5	49 ± 1	7 ± 1	47 ± 1	39 ± 1
sPPBu5	13.6	250	186 ± 5	39 ± 2	7 ± 2	46 ± 6	35 ± 2
sPPBu5	13.6	450	286 ± 10	42 ± 3	4 ± 2	44 ± 2	37 ± 1
sPPBu6	18.2	250	170 ± 3	29 ± 1	4 ± 1	38 ± 4	28 ± 2
sPPBu6	18.2	450	286 ± 8	42 ± 3	7 ± 2	46 ± 4	31 ± 5
sPPBu7	31.5	250	171 ± 1	29 ± 2	3.4 ± 0.3	19 ± 5	14 ± 1
sPPBu7	31.5	450	273 ± 3	47 ± 1	9 ± 3	36 ± 8	25 ± 5
sPPBu8	37.9	250	174 ± 11	28 ± 3	1.5 ± 0.9	32 ± 3	27 ± 4
sPPBu8	37.9	450	281 ± 2	44 ± 1	2 ± 1	27 ± 1	21 ± 1
sPPBu9	51.7	300	176 ± 10	51 ± 3	5 ± 1	38 ± 5	21 ± 2
sPPBu9	51.7	450	253 ± 7	56 ± 3	8 ± 4	26 ± 3	12 ± 1
sPPBu10	52.1	300	207 ± 13	30 ± 3	0.8 ± 0.2	18 ± 2	14 ± 2
sPPBu10	52.1	450	253 ± 7	56 ± 3	6.0 ± 0.1	30 ± 2	20 ± 3
sPPBu11	69.9	400	253 ± 10	40 ± 4	3 ± 2	0	0
sPPBu12	89	450	329 ± 22	33.6 ± 0.4	3 ± 2	0	0

[a] The tension set of stress-relaxed fibers measured at the end of the hysteresis cycles successive to the I cycle are null.

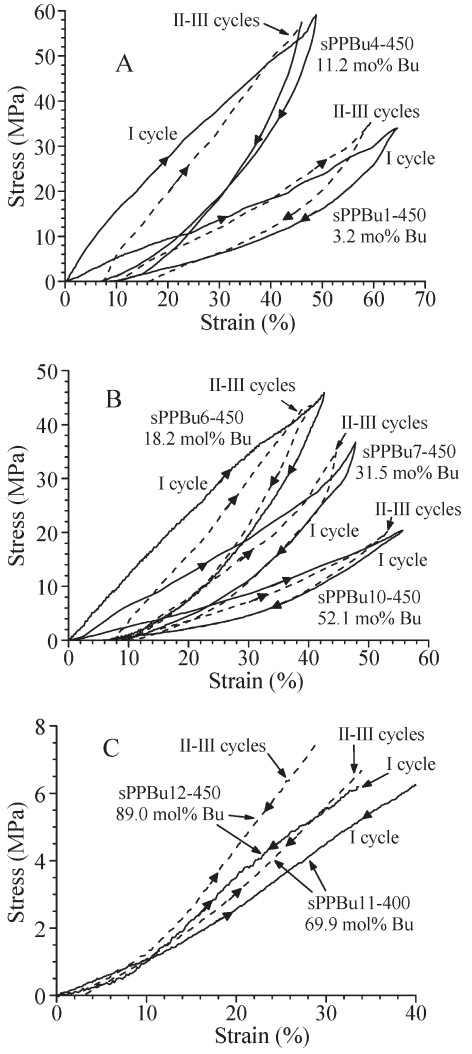

Figure 10. Stress−strain hysteresis cycles composed of the stretching and relaxation steps (at controlled rate) according to the direction of the arrows of stress-relaxed oriented fibers sPPBu1-450 and sPPBu4-450 (A), sPPBu6-450, sPPBu7-450, and sPPBu10-450 (B), sPPBu11-400 and sPPBu12-450 (C). In (C) for the fibers sPPBu11-400 and sPPBu12-450 the curves corresponding to the stretching and relaxation steps are coincident (null hysteresis). The first cycles (continuous lines) and curves averaged over the successive II and III cycles (dashed lines) are reported. The stress-relaxed fibers have been prepared by stretching compression-molded films of the samples sPPBuN with N = 1, 4, 6, 7, 10, and 12 at 450% deformation (final length $L_f = 5.5L_0$, with L_0 the initial length of the compression-molded film) and at 400% deformation (final length $L_f = 5L_0$) for the samples sPPBu11 and then removing the tension.

draw plateau (Figure 8A−C), as in stress−strain curves of the crystalline samples. In particular, the yield stress of the sample sPPBu7 at $x_c = 0$ (Figure 8A) is close to that of the crystalline sample sPPBu11 at $x_c = 25\%$ (Figure 8E). This is probably due to the fact that for the samples sPPBu7−sPPBu9 with butene content in the range 30−50 mol % the crystallization is very fast under the applied stress, and probably, a large part of the total crystallinity produced during stretching is achieved already at very small deformations before the draw plateau. A demonstration of the crystallization during stretching is given in Figure 9 that reports the X-ray diffraction profiles of compression-molded films of the samples sPPBu7−sPPBu10 before stretching and at the end of the stress−strain tests of Figure 8, after having cut the stretched samples in small pieces in order to achieve random orientation of crystals. It is apparent that the starting amorphous films are all crystallized after stretching up to the breaking.

Mechanical Properties of Oriented Fibers. Oriented fibers of sPPBu copolymers have been prepared by stretching compression-molded films of initial length L_0 up to values of deformation ε_{max}, ranging from 250% to 450% (final lengths L_f comprised in the range $3.5L_0-5.5L_0$) and then removing the tension allowing the relaxation of the films up to the relaxed length L_r (samples sPPBuN-ε_{max}). The values of the maximum deformation ε_{max} and the corresponding values of tension set and the elastic recovery are reported in Table 3, whereas the corresponding values of the percentage of recovered strain $R(\varepsilon)$ after releasing the tension are shown in Figure 7E.

The stress−strain hysteresis cycles, composed of the curves recorded during the stretching and the successive relaxation, of some stress-relaxed oriented fibers sPPBuN-450 (or sPPBuN-400) are reported in Figure 10. In these cycles stress-relaxed oriented fibers of initial length L_r are stretched up to the final length L_f ($L_f = 5.5L_0$ or $5L_0$), that is, up to the maximum length achieved during the stretching of the starting unoriented film used for the preparation of the fibers (ε_{max} = 450% or 400%), so that the maximum deformation achieved during the first cycle ($\varepsilon = 100(L_f - L_r)/L_r$) for each sample is numerically equal to the elastic recovery $r(\varepsilon_{max})$ of the unoriented film reported in Table 3. For each oriented film at least three consecutive hysteresis cycles have been recorded; each cycle has been performed 10 min after the end of the previous cycle. The values of tension set and the values of percentage of dissipated energy during each cycle are reported in Table 3.

It is apparent from Figure 10 and the data of Table 3 that for all samples the values of the tension set after the first hysteresis cycle are already very small (less than 10%) and zero after the successive cycles, the successive stress−strain curves being coincident. Furthermore, the stress−strain curves of stress-relaxed fibers sPPBuN-450 with $N < 11$ (i.e., with butene content lower than 69 mol %) present non-null hysteresis (Figure 10A,B), the values of the percentage of dissipated energy being lower than 47% for the first cycle, and tend to decrease for the successive cycles, achieving values lower than 39%. The stress-relaxed fibers sPPBu11-400 and sPPBu12-450 (with butene content higher than 69 mol %) show, instead, negligible hysteresis (Figure 10C). These data indicate that, regardless of the value of maximum deformation ε_{max} achieved for the preparation of the stress-relaxed fibers, all fiber samples show good elastic properties in a nontrivial deformation range comprised between 40% and 70%. The good elastic behavior of the unoriented films is improved in the oriented fibers.

This is due to the fact that once the samples have experienced irreversible plastic deformation during stretching of unoriented specimens that limits the elastic performance of compression-molded unoriented films, and a high degree of crystal orientation has been achieved,[25] the deformation of the so-obtained oriented fibers may be completely recovered. However, a decrease of the values of stress and of the range of elastic strain is observed for the samples with highest butene content (Figure 10C).

As demonstrated in our previous paper,[25] the plastic deformation and the elastic recovery of sPPBu samples are associated with the occurrence of polymorphic transitions during stretching and relaxation. A scheme of the transformations induced by stretching and relaxation is shown in Figure 11. In samples with butene content lower than 20 mol % the helical form I of sPP transforms by stretching into the trans-planar form III (Figure 11A,B), whereas no

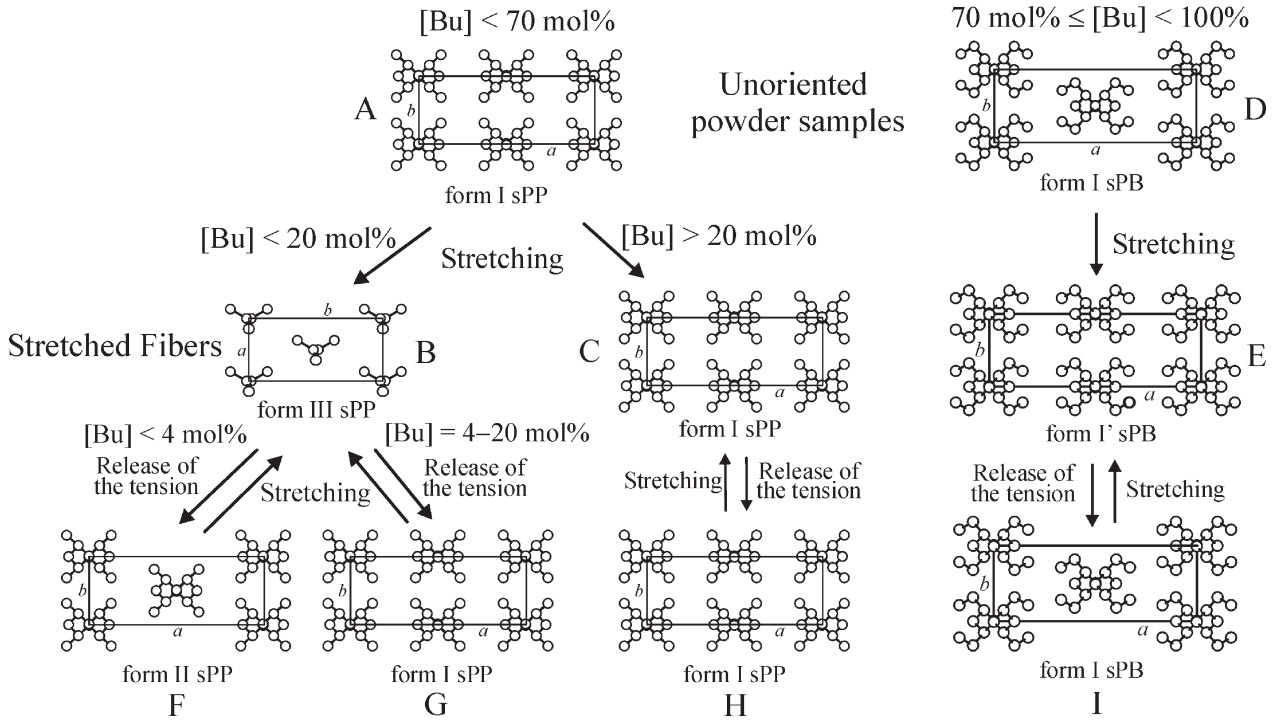

Figure 11. Scheme of the polymorphic transitions occurring during plastic deformation of unoriented melt-crystallized samples of sPPBu copolymers and during stretching and relaxation by releasing the tension of oriented fibers of the copolymers, for different ranges of comonomer concentration.

transformation is observed in samples with butene content higher than 20 mol % (Figure 11C).[25] In samples with butene content higher than 69 mol % the *C*-centered helical form I of sPB that crystallize in the powder samples (Figure 11D) transforms into the *B*-centered form I′ of sPB by stretching at high deformations (Figure 11E).[25] The trans-planar form III obtained by stretching (Figure 11B) transforms into the helical form II (Figure 11F) or in the helical form I of sPP (Figure 11G) during relaxation and elastic recovery of samples with butene contents lower than 4 mol % (sample sPPBu1-450 of Figure 10A) or in the range 4−20 mol % (samples sPPBu2−sPPBu6), respectively.[25] These phase transitions are reversible (Figure 11B,F,G) and the oriented samples show elastic behavior (Figure 10A). As in the case of sPP homopolymer,[6] it may be inferred that the polymorphic transition between the helical form II and the trans-planar form III provides an enthalpic contribution to the elasticity of sPPBu copolymers having low butene concentration. We recall that in the case of sPP the value of $\Delta H_{II-III} = 2.6$ kJ/mol of monomeric unit for the enthalpy difference associated with this reversible phase transition has been evaluated, in agreement with the difference between the calculated energy of the two polymorphic forms.[26] This experimental determination provided a definitive demonstration of the property of some crystalline polymers to respond immediately to applied stress through a crystal−crystal phase transition, which accounts for the macroscopic recovery of the dimensions of the sample upon releasing the applied tension.

Oriented fibers of sPPBu samples with butene concentrations higher than 20 mol % show similar elastic properties (samples sPPBu7−sPPBu10 in Figure 10B), which are not associated with polymorphic transformations (Figure 11C−H),[25] and have, therefore, a purely entropic origin. The defective crystals of form I of sPP present in these sPPBu samples merely act as physical knots of the elastomeric network, preventing the viscous flow of the chains.

Oriented fibers of samples with butene concentration higher than 69 mol % also show elastic behavior (Figure 10C), which

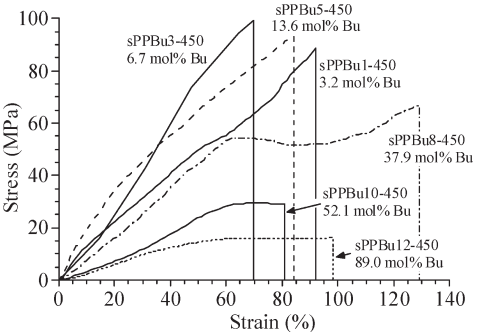

Figure 12. Stress−strain curves of stress-relaxed fibers sPPBuN-ε_{max} prepared by stretching compression-molded unoriented films of sPPBu copolymer samples of the indicated butene (Bu) concentration up to a maximum deformation ε_{max} and then releasing the tension. Each fiber is tested after having experienced at least three consecutive hysteresis cycles of the kind of Figure 10.

is again associated with the transformation of the helical form I′ of sPB, formed by stretching, into the more stable *C*-centered helical form I of sPB (Figure 11E,I).[25] This transformation probably provides a small energetic contribution to the elasticity of these samples, even though the entropic factor due to the stretching and recoiling of the chains belonging to the amorphous network plays the main role.

The stress−strain curves of the stress-relaxed fibers sPPBuN-ε_{max} of sPPBu copolymers that have experienced at least three consecutive hysteresis cycles of the kind of Figure 10 are reported in Figure 12. The Young modulus and the stress and strain at break evaluated from the stress−strain tests of Figure 12 are reported in Table 4. It is apparent that the stress-relaxed fibers sPPBuN-ε_{max} exhibit a dramatic increase of mechanical strength with respect to the corresponding unoriented films, regardless of the value of ε_{max} achieved for their preparation. The values of tension set at break of the oriented fibers are zero, indicating a perfect elastic recovery after breaking. Furthermore, these fibers

Table 4. Young Modulus (E), Strain (ε_b) and Stress at Break (σ_b), and Tension Set at Break (t_b) of Stress-Relaxed Fibers of sPPBu Samples

stress-relaxed fibers	butene (mol %)	ε_{max} (%)	E (MPa)	ε_b (%)	σ_b (MPa)	t_b (%)
sPPBu1-450	3.2	450	127 ± 29	91 ± 12	89 ± 15	0
sPPBu3-450	6.7	450	149 ± 25	70 ± 16	99 ± 19	0
sPPBu4-250	11.2	250	127 ± 7	167 ± 7	56 ± 12	0
sPPBu4-450	11.2	450	132 ± 22	60 ± 11	88 ± 24	0
sPPBu5-250	13.6	250	98 ± 9	162 ± 17	57 ± 8	0
sPPBu5-450	13.6	450	155 ± 10	84 ± 10	93 ± 13	0
sPPBu6-250	18.2	250	63 ± 13	169 ± 13	43 ± 5	0
sPPBu6-450	18.2	450	100 ± 11	65 ± 3	79 ± 14	0
sPPBu7-250	31.5	250	38 ± 5	186 ± 7	28 ± 2	0
sPPBu7-450	31.5	450	53 ± 21	108 ± 11	62 ± 8	0
sPPBu8-250	37.9	250	45 ± 7	191 ± 14	33 ± 5	0
sPPBu8−450	37.9	450	40 ± 6	129 ± 11	66 ± 2	0
sPPBu9-300	51.7	300	30 ± 3	200 ± 15	29 ± 4	0
sPPBu9-450	51.7	450	18 ± 2	145 ± 76	20 ± 4	0
sPPBu10-300	52.1	300	29 ± 3	139 ± 41	24 ± 4	0
sPPBu10-450	52.1	450	23 ± 2	81 ± 21	29 ± 3	0
sPPBu11-400	69.9	400	7 ± 2	71 ± 13	12 ± 4	0
sPPBu12-450	89	450	11 ± 2	98 ± 15	16.1 ± 0.1	0

achieve values of Young modulus much higher than those of the corresponding unoriented specimens (Figure 7A).

The neat increase of rigidity and mechanical strength of the oriented fibers is due to the fact that a high degree of orientation of the crystals with chain axes parallel to the stretching direction is achieved by stretching compression-molded samples already at low deformations (≈200%), and this high degree of orientation is maintained after releasing the tension.[25] These data indicate that oriented fibers of sPPBu copolymers show very good elastic behavior that is associated with remarkable values of rigidity and mechanical strength due to the non-negligible level of crystallinity.

Conclusions

A novel class of thermoplastic elastomeric materials, based on syndiotactic propylene−butene copolymers (sPPBu), have been synthesized with a C_s-symmetric syndiospecific metallocene catalyst. These copolymers crystallize in the whole range of comonomer composition in disordered modification intermediate between the stable antichiral *B*-centered form I of sPP and the isochiral *C*-centered form I of sPB. Propene and butene cocrystallize at any comonomer concentration and are included in the crystalline lattice of sPB and sPP, respectively.

Melt-crystallized unoriented samples of all sPPBu copolymers show good elastic properties, which are improved in oriented fibers, with remarkable rigidity and mechanical strength due to the non-negligible level of crystallinity that is maintained at any comonomer concentration.

For the more crystalline samples with low butene concentration the elastic properties are associated with reversible polymorphic transformations that occur during the processes of stretching and elastic recovery of fibers. The occurrence of these reversible phase transitions assists the elasticity of sPPBu copolymers with butene content lower than 20 mol %, through a non-negligible free energy contribution.

In the case sPPBu samples with butene content higher that 20 mol %, no stress-induced phase transition occurs, and the defective crystals of form I of sPP merely act as physical knots of the elastomeric network, preventing the viscous flow of the chains, as in the case of conventional thermoplastic elastomers.

These crystallization properties are responsible for the development of the outstanding mechanical properties of sPPBu copolymers, which provide a variety of elastomeric materials characterized by values of stiffness and mechanical strength that may be tuned by simply changing the comonomer concentration.

Acknowledgment. Financial support from INSTM (Prisma project 2007) is gratefully acknowledged.

References and Notes

(1) Coates, G. W.; Waymouth, R. M. *Science* **1995**, *267*, 217.
(2) (a) Mallin, D. T.; Rausch, M. D.; Lin, Y. G.; Dong, S.; Chien, J. C. W. *J. Am. Chem. Soc.* **1990**, *112*, 2030. (b) Bravakis, A. M.; Bailey, L. E.; Pigeon, M.; Collins, S. *Macromolecules* **1998**, *31*, 1000. (c) Muller, G.; Rieger, B. *Prog. Polym. Sci.* **2002**, *27*, 815. (d) De Rosa, C.; Auriemma, F.; Perretta, C. *Macromolecules* **2004**, *37*, 6843.
(3) Toki, S.; Sics, I.; Burger, C.; Fang, D.; Liu, L.; Hsiao, B. S.; Datta, S.; Tsou, A. H. *Macromolecules* **2006**, *39*, 3588.
(4) (a) Tian, J.; Hustad, P. D.; Coates, G. W. *J. Am. Chem. Soc.* **2001**, *123*, 5134. (b) Ruokolainen, J.; Mezzenga, R.; Fredrickson, G. H.; Kramer, E. J.; Hustad, P. D.; Coates, G. W. *Macromolecules* **2005**, *38*, 851. (c) Furuyama, R.; Mitani, M.; Mohri, J.; Mori, R.; Tanaka, H.; Fujita, T. *Macromolecules* **2005**, *38*, 1546.
(5) (a) Arriola, D. J.; Carnahan, E. M.; Hustad, P. D.; Kuhlman, R. L.; Wenzel, T. T. *Science* **2006**, *312*, 714. (b) Wang, H. P.; Khariwala, D. U.; Cheung, W.; Chum, S. P.; Hiltner, A.; Baer, E. *Macromolecules* **2007**, *40*, 2852.
(6) (a) De Rosa, C.; Auriemma, F. *Prog. Polym. Sci.* **2006**, *31*, 145. (b) De Rosa, C.; Auriemma, F.; Ruiz, O. *Chem. Mater.* **2006**, *18*, 3523. (c) Auriemma, F.; De Rosa, C.; Esposito, S.; Mitchell, G. R. *Ang. Chem., Int. Ed.* **2007**, *46*, 4325.
(7) (a) Kakugo, M. *Macromol. Symp.* **1995**, *89*, 545. (b) Naga, N.; Mizunuma, K.; Sadatoshi, H.; Kakugo, M. *Macromolecules* **1997**, *30*, 2197. (c) Naga, N.; Mizunuma, K.; Sadatoshi, H.; Kakugo, M. *Polymer* **2000**, *41*, 203.
(8) (a) Thomann, R.; Kressler, J.; Mulhaupt, R. *Macromol. Chem. Phys.* **1997**, *198*, 1271. (b) Thomann, R.; Kressler, J.; Mulhaupt, R. *Polymer* **1998**, *39*, 1907. (c) Jungling, S.; Mulhaupt, R.; Fisher, D.; Langhauser, F. *Angew. Makromol. Chem.* **1995**, *229*, 93.
(9) Hauser, G.; Schmidtke, J.; Strobl, G. *Macromolecules* **1998**, *31*, 6250.
(10) (a) Arranz-Andrés, J.; Guevara, J. L.; Velilla, T.; Quijada, R.; Bonavente, R.; Pérez, E.; Cerrada, M. L. *Polymer* **2005**, *46*, 12287. (b) Quijada, R.; Guevara, J. L.; Galland, G. B.; Rabagliati, R. M.; Lopez-Majada, J. M. *Polymer* **2005**, *46*, 1567.
(11) (a) Seraidaris, T.; Kaminsky, W.; Seppala, J. V.; Lofgren, B. *Macromol. Chem. Phys.* **2005**, *206*, 1319. (b) Rulhoff, S.; Kaminsky, W. *Macromol. Chem. Phys.* **2006**, *207*, 1450.
(12) Schwerdtfeger, E. D.; Miller, S. A. *Macromolecules* **2007**, *40*, 5662.
(13) (a) De Rosa, C.; Auriemma, F. *Adv. Mater.* **2005**, *17*, 1503. (b) De Rosa, C.; Auriemma, F. *Macromolecules* **2006**, *39*, 249. (c) De Rosa, C.; Auriemma, F.; Fanelli, E.; Talarico, G.; Capitani, D. *Macromolecules* **2003**, *36*, 1850.
(14) De Rosa, C.; Talarico, G.; Caporaso, L.; Auriemma, F.; Galimberti, M.; Fusco, O. *Macromolecules* **1998**, *31*, 9109.
(15) Chatani, Y.; Maruyama, H.; Noguchi, K.; Asanuma, T.; Shiomura, T. *J. Polym. Sci., Part C* **1990**, *28*, 393.
(16) Corradini, P.; Natta, G.; Ganis, P.; Temussi, P. A. *J. Polym. Sci., Part C* **1967**, *16*, 2477.
(17) Lotz, B.; Lovinger, A. J.; Cais, R. E. *Macromolecules* **1988**, *21*, 2375.
(18) Lovinger, A. J.; Lotz, B.; Davis, D. D.; Padden, F. J. *Macromolecules* **1993**, *26*, 3494.

(19) (a) De Rosa, C.; Venditto, V.; Guerra, G.; Corradini, P. *Makromol. Chem.* **1992**, *193*, 1351. (b) De Rosa, C.; Venditto, V.; Guerra, G.; Pirozzi, B.; Corradini, P. *Macromolecules* **1991**, *24*, 5645.
(20) Ewen, J. A.; Jones, R. L.; Razavi, A.; Ferrara, J. D. *J. Am. Chem. Soc.* **1988**, *110*, 6255.
(21) (a) Herrmann, W. A.; Rohrmann, J.; Herdtweck, E.; Spaleck, W.; Winter, A. *Angew. Chem., Int. Ed.* **1989**, *28*, 1511. (b) Razavi, A.; Atwood, J. L. *J. Organomet. Chem.* **1993**, *459*, 117.
(22) Ray, G. I.; Johnson, P. E.; Knox, J. R. *Macromolecules* **1977**, *10*, 773.
(23) Brandrup, L.; Immergut, E. H.; Grulke, E. A. *Polymer Handbook*; John Wiley: New York, 1999.
(24) De Rosa, C.; Auriemma, F.; Vinti, V. *Macromolecules* **2007**, *30*, 4137.
(25) De Rosa, C.; Auriemma, F.; Corradi, M.; Caliano, L.; Talarico, G. *Macromolecules* **2008**, *41*, 8712.
(26) Palmo, K.; Krimm, S. *Macromolecules* **2002**, *35*, 394.